We are IntechOpen,
the world's leading publisher of
Open Access books
Built by scientists, for scientists

6,900
Open access books available

186,000
International authors and editors

200M
Downloads

154
Countries delivered to

Our authors are among the

TOP 1%
most cited scientists

12.2%
Contributors from top 500 universities

BOOK CITATION INDEX
CLARIVATE ANALYTICS
INDEXED

WEB OF SCIENCE™

Selection of our books indexed in the Book Citation Index
in Web of Science™ Core Collection (BKCI)

Interested in publishing with us?
Contact book.department@intechopen.com

Numbers displayed above are based on latest data collected.
For more information visit www.intechopen.com

Robust Diagnosis by Observer Using the Bond Graph Approach

Abderrahmène Sallami

Additional information is available at the end of the chapter

Abstract

In this chapter, we have proposed a Luenberger observer linear systems diagnostic technique using the bond graph. Indeed, an observer can reconstruct or estimate the current state of a real system using the available measurements, without prior knowledge of the initial conditions. In addition, it allows to estimate the nonmeasurable states of a system. The design of the observer is carried out using graphical methods from the structural properties of the model bond graph becomes simple and practical to build. We presented the bond graph approach for the construction of a full-order observer and proposed a new BG-based observer diagnostic method. Subsequently, we presented the uncertain parameter systems modeled by the bond graph approach, and we also proposed a new method for diagnosing systems with uncertain parameters by Luenberger observer. In the last part of this chapter, we developed and proposed an observer bench diagnosis technique (BG-DOS/BG-GOS) to detect and locate defects.

Keywords: robust diagnosis, bond graph, Luenberger observer, DC motor, generation of robust residues

1. Introduction

Nowadays, the engineering sciences rely heavily on the estimation of the state of the systems. Indeed, the complete knowledge of the state of a system is often necessary for the elaboration of a control law or the setting up of a strategy of monitoring or diagnosis. In practice, the state of a system is not always available and the input and output signals are the only quantities accessible by measurement. The most widespread solution to this problem consists in coupling to the system another auxiliary system, called estimator or observer of state. The observer

provides an estimate of the state of the system based on its model and measurements of its inputs and outputs. The observer conventionally used, within the framework of linear systems, is said to have proportional gain or Luenberger. In recent years, observer diagnosis is used to estimate shareholder defects and sensor defects [1].

In this chapter, we show how the leap graph model can be used for modeling, simulation and residual determination by Luenberger observers for diagnosis system.

2. Observer diagnosis

2.1. Observational diagnosis using the analytical model

The principle of diagnosis consists in estimating, by appropriate techniques, all the components of the state vector or, more generally, the output of the process, using the error of estimation as a residue [2].

This operation is carried out by means of a proportional observer. The functional diagram of such a method is given in **Figure 1**.

The residue equations are defined as follows:

State estimation residue:

$$r_x = \tilde{X} = x - \hat{x} \tag{1}$$

Exit estimate residue:

$$r_y = \tilde{Y} = y - \hat{y} = C(x - \hat{x}) \tag{2}$$

2.1.1. Residual in the case of normal operation

We consider a linear system whose equations of states are defined as follows:

$$\begin{cases} \dot{x}(t) = Ax(t) + Bu(t) \\ y(t) = Cx(t) \end{cases} \tag{3}$$
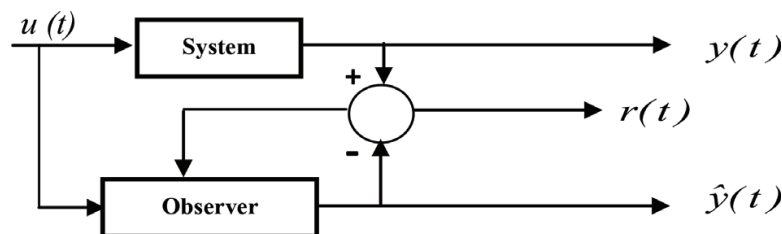

Figure 1. Observational diagnosis.

The proportional state observer is defined by equations:

$$\begin{cases} \dot{\hat{x}}(t) = A\hat{x}(t) + Bu(t) + K(y - \hat{y}) \\ \hat{y}(t) = C\hat{x}(t) \end{cases} \tag{4}$$

The state estimation or state reconstruction residual is by definition:

$$r_x = \tilde{X} = x - \hat{x} \tag{5}$$

For a proportional observer, the evolution of the residue r(t) is:

$$\dot{r}_x = (A - KC)r_x \tag{6}$$

The Laplace transform of Eq. (6) is written:

$$r_x(p) = (pI - A + KC)^{-1}r_0 \tag{7}$$

The output reconstruction residue is defined by:

$$r_y = \tilde{Y} = y - \hat{y} = C(x - \hat{x}) = C\tilde{X} = Cr_x \tag{8}$$

Hence using the previous result, Eq. (8) is written:

$$r_y(p) = C(pI - A + KC)^{-1}r_0 \tag{9}$$

2.1.2. Residual with a sensor failure

We consider again the same linear system in which the measurements made are subjected to a defect which we denote by fc(t) of unknown amplitude and appearing at an unknown time (**Figure 2**):
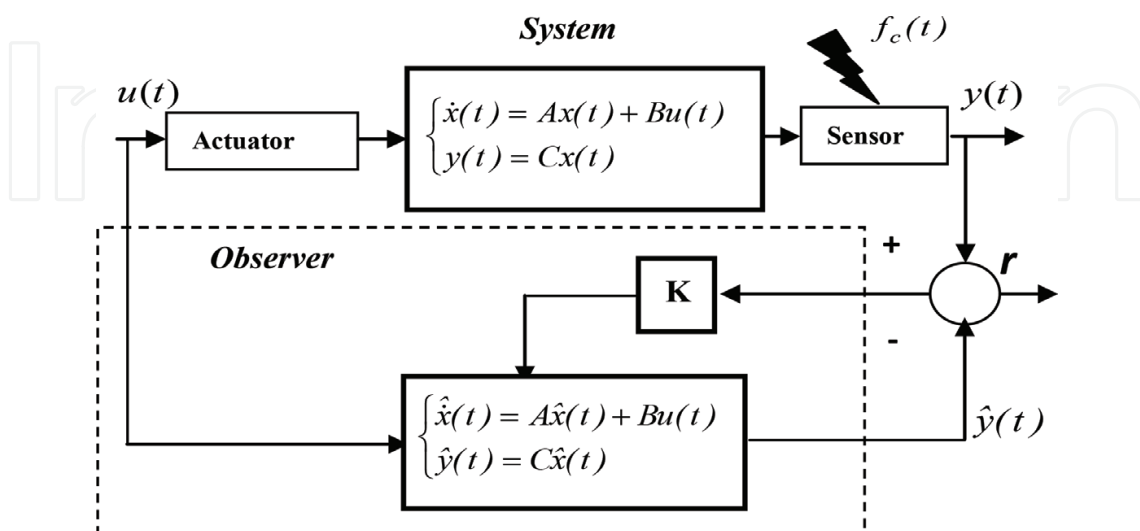

Figure 2. Proportional observer with sensor fault.

The equations of states become:

$$\begin{cases} \dot{x}(t) = Ax(t) + Bu(t) \\ y(t) = Cx(t) + Ff_c(t) \end{cases} \tag{10}$$

In order to diagnose the state of operation of the system, the states reconstruct or must be sensitive to this bias and must highlight this sensor defect, isolate it and possibly quantify it. The residue r(t) is:

$$\dot{r}_x(t) = (A - KC)r_x(t) + Ff_c(t) \tag{11}$$

The equation is written using the Laplace transformation:

$$r_x(p) = (pI - A + KC)^{-1}\big(r_0 + Ff_c(p)\big) \tag{12}$$

To see the error of reconstruction of output according to the biases of the sensors, we do not take into account the initial conditions of or:

$$r_x(p) = \Big[I - C(pI - A + KC)^{-1}K\Big]Ff_c(p) \tag{13}$$

2.1.3. Residual with an actuator failure

In the case where the control applied to the system is misinterpreted by the actuator, the latter introduces a fault which we denote by $f_a(t)$ (**Figure 3**).

The equation describing the faulty system is:

$$\begin{cases} \dot{x}(t) = Ax(t) + Bu(t) + Df_a(t) \\ y(t) = Cx(t) + Ff_c(t) \end{cases} \tag{14}$$

For zero initial conditions, the expression of the state reconstruction residue is of the form:

$$r_x(p) = \Big[I - C(pI - A + KC)^{-1}K\Big]Ff_c(p) + C(pI - A + KC)^{-1}Df_a(p) \tag{15}$$
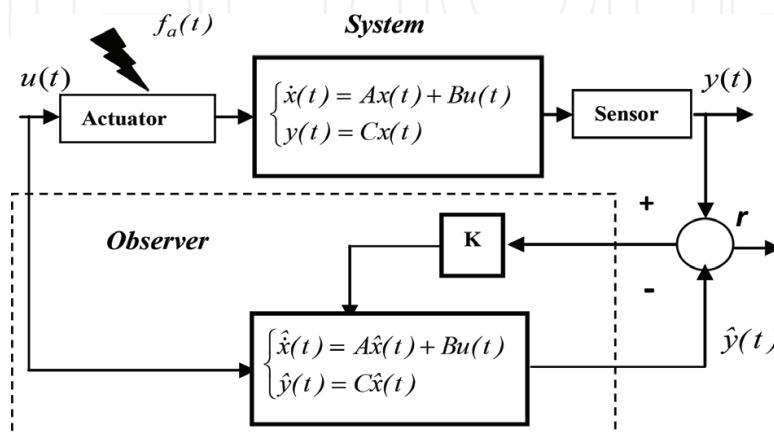

Figure 3. Proportional observer with actuator fault.

The output reconstruction residue is defined by equation:

$$r_x(p) = C(pI - A + KC)^{-1} Df_a(p) \tag{16}$$

2.1.4. Residual with sensor and actuator failures

In this case, we have the addition of two defects at the system level:

- Fault at sensor *fc(t)*;

- Fault at actuator *fa(t)*.

The equations of the system are then written as follows:

$$\begin{cases} \dot{x}(t) = Ax(t) + Bu(t) + Df_a(t) \\ y(t) = Cx(t) + Ff_c(t) \end{cases} \tag{17}$$

Applying the principle of superposition, since the system is linear, we can determine the output reconstruction residue which is the sum of the residuals caused by the sensor alone and the actuator alone. The expression of this residue is as follows:

$$r_x(p) = \left[I - C(pI - A + KC)^{-1}K \right] Ff_c(p) + C(pI - A + KC)^{-1}Df_a(p) \tag{18}$$

This residue is sensitive to sensor and actuator defects.

2.2. Observational diagnosis using the bond graph model

2.2.1. Construction of a Luenberger observer based on model bond graph

To construct the observers, one must check the observability of the system. From a Bond Graph perspective, proposed by [3], a system modeled by leap graph is structurally observable, if the following two conditions are met:

- *First condition*: There is at least one causal path linking a sensor to each dynamic element I or C in the integral causality when the hop graph is the preferred integral causal model.

- *Second condition*: All elements I or C admitting a derivative causality when we put the leap graph model in derivative causality, and dualize the sensors.

Figure 4 presents, respectively, the proportional observer using the bond graph for elements I and C [4].

2.2.2. Proportional observer diagnosis using the bond graph model

The observer provides an estimate of the state of the system based on its model and measurements of its inputs and outputs. The observer conventionally used in linear systems is said to have Proportional (P) or Luenberger gain [5].

Consider a continuous system described by the equation of state using the hop graph represented in **Figure 5**:
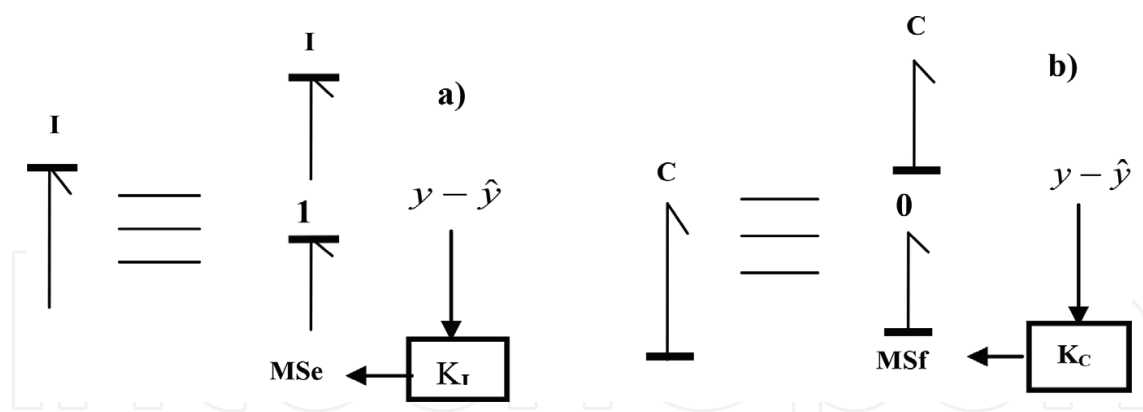
Figure 4. Construction of a proportional observer case of: (a) element I and (b) element C.
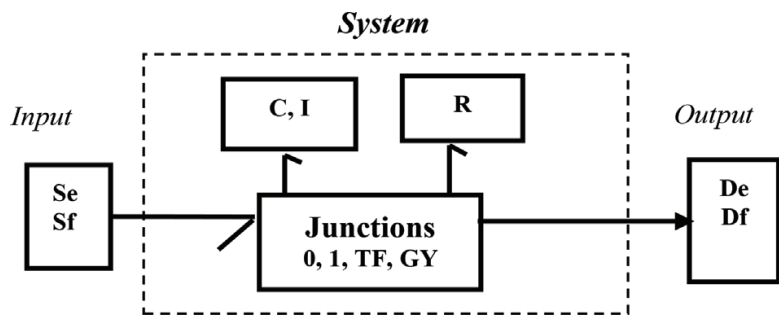

Figure 5. Schema of the continuous system described by bond graph.
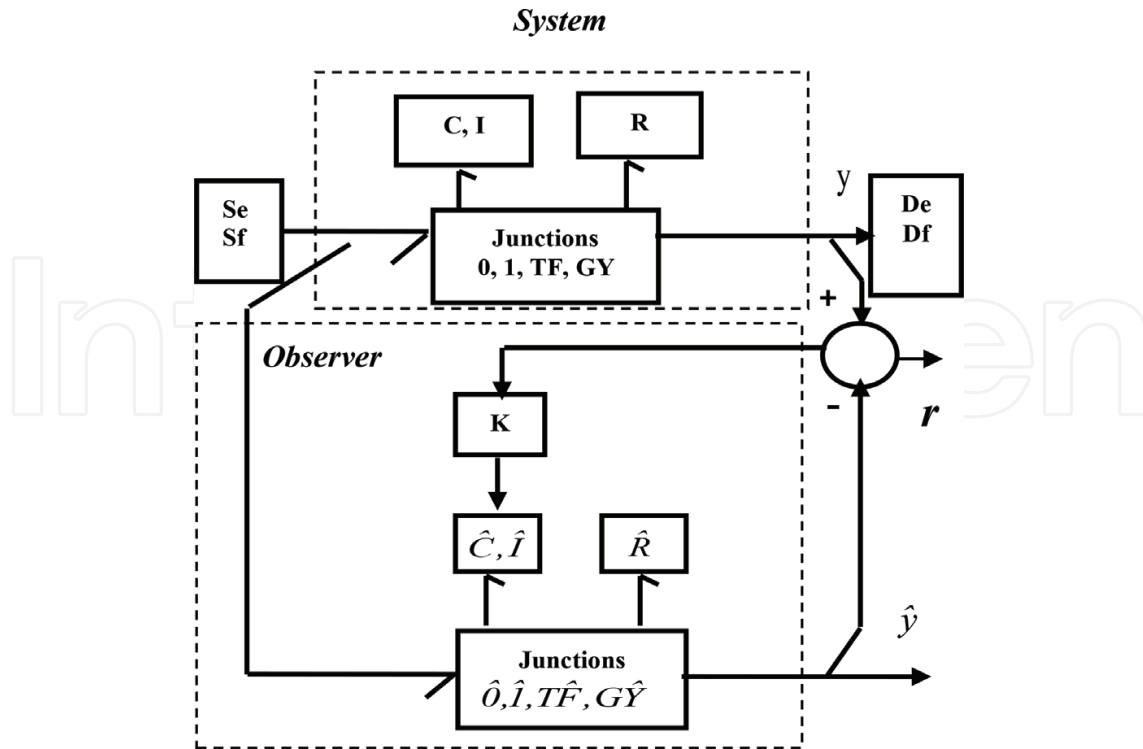

Figure 6. Structure of a Luenberger observer using graph graph.

The state observer of proportional type is represented by **Figure 6**. The equation of state is of the following form:

$$\begin{cases} \dot{\hat{x}}(t) = \begin{pmatrix} \dot{\hat{p}}_I \\ \dot{\hat{q}}_c \end{pmatrix} = A \begin{pmatrix} p_L \\ q_C \end{pmatrix} + Bu(t) + K(y(t) - \hat{y}(t)) \\ \hat{y} = C \begin{pmatrix} \hat{p}_L \\ \hat{q}_C \end{pmatrix} \end{cases}$$

2.2.3. Generation of residues

The generation of residues from a proportional observer using the bond graph model is summarized by the following steps:

Verify that the bond graph model of the system is structurally observable, if so, then continue the next steps;

Construction of the observer using the graph;

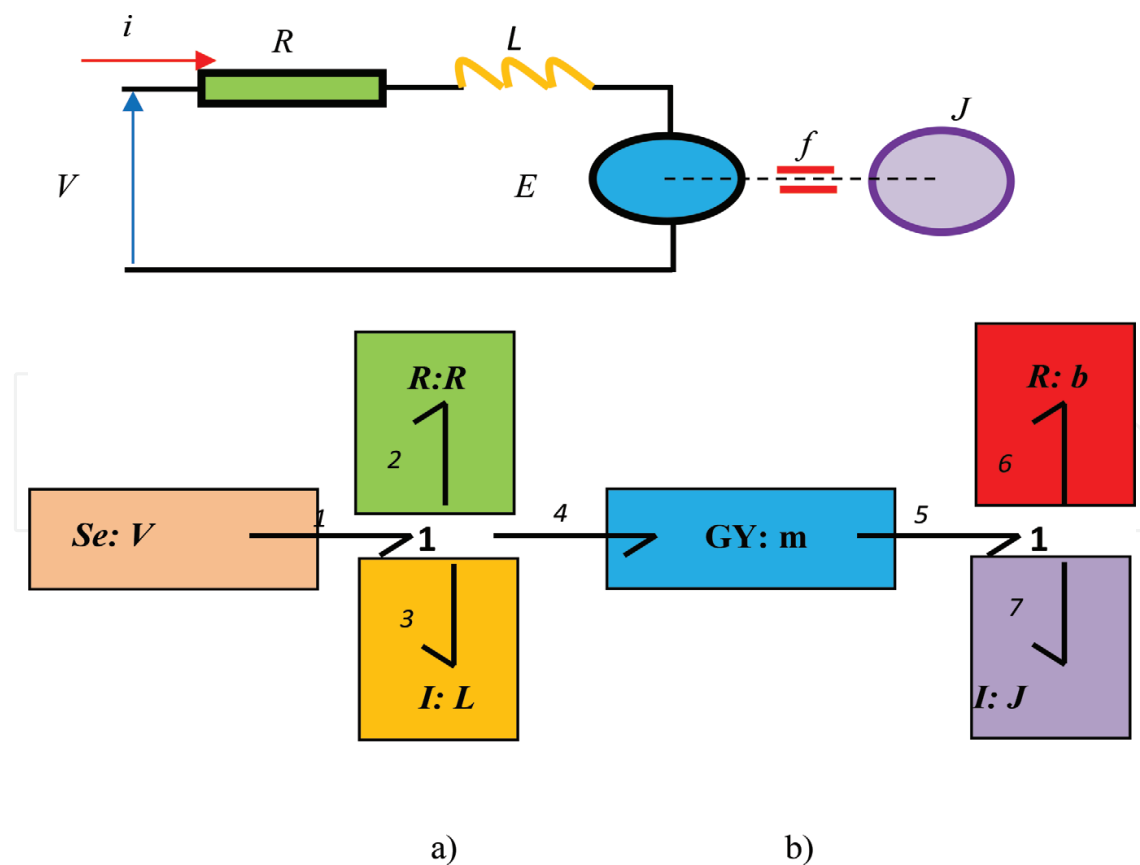The symbolic expression of residue is deduced from equation:

a)   b)

Figure 7. (a): Direct current motor, (b): Bond model of the DC motor.

$$r = \dot{y} - \hat{y} \tag{19}$$

After calculation, the residue is in the form:

$$r : \Phi\left(R, I, C, TF, GY\right) \tag{20}$$

2.3. Determination of the gain of the Luenberger observer

2.3.1. Determination of the gain of the Luenberger observer by the analytical method

To guarantee the asymptotic convergence toward zero of the estimation error, choose the gain K to stabilize the matrix (A-KC).

The gain K can be determined by two methods:

- Placement of the poles: This method makes it possible to have a stable observer and allows playing on the criterion of rapidity of the convergence of the observer by choosing eigenvalues greater or less in absolute values.

- LYAPUNOV criterion: This method guarantees the stability of the observer but gives no idea about the speed of convergence of the observer since it does not allow to choose the eigenvalues.

2.3.2. Determination of the gain of the Luenberger observer by the bond graph method

First, we will compute the coefficients of the characteristic polynomial of the linear system:

$$p_A = p^n + a_1 \cdot p^{n-1} + \ldots\ldots + a_{n-1} \cdot p + a_n \tag{21}$$

The calculation of the gain of the observer by leap graph is based on the Rahmani theorem, [6].

Theorem: The value of each coefficient (ai) of the characteristic polynomial PA isequal to the total gain of families of causation cycles of order i of the model graph graph:

The gain of each affected family of causality cycles must be multiplied by (-1) d if the family is constituted by disjoint causality cycles.

2.4. Example

Consider the electrical system of a DC motor and its model bond graph given in **Figure 7**. On this system, we will detect and locate faults at the flow sensors (speed sensor Df_1 and current sensor Df_2).

2.4.1. State equation

The equation of state of the DC motor is as follows:

$$\begin{cases} \begin{pmatrix} \dot{p}_3 \\ \dot{p}_7 \end{pmatrix} = \begin{bmatrix} -\dfrac{R}{L} & -\dfrac{m}{J} \\ \dfrac{m}{L} & -\dfrac{b}{J} \end{bmatrix} \begin{pmatrix} p_3 \\ p_7 \end{pmatrix} + \begin{bmatrix} 1 \\ 0 \end{bmatrix} U \\ \\ y = \begin{bmatrix} \dfrac{1}{L} & 0 \\ 0 & \dfrac{1}{J} \end{bmatrix} \begin{pmatrix} p_3 \\ p_7 \end{pmatrix} \end{cases} \tag{22}$$

With R: armature resistance, L: armature inductance, m: torque coefficient, J: moment of inertia, b: coefficient of friction.

R = 1 Ω; L = 5 mH; b = 10^{-4} Nm/rd. S^{-1}; J = 10^{-3} Kg.m^2, m = 0.2 Nm/A.

$$\begin{cases} \begin{pmatrix} \dot{p}_3 \\ \dot{p}_7 \end{pmatrix} = \begin{bmatrix} -200 & -200 \\ 40 & -0.1 \end{bmatrix} \begin{pmatrix} p_3 \\ p_7 \end{pmatrix} + \begin{bmatrix} 1 \\ 0 \end{bmatrix} U \\ \\ y = \begin{bmatrix} 200 & 0 \\ 0 & 1000 \end{bmatrix} \begin{pmatrix} p_3 \\ p_7 \end{pmatrix} \end{cases}$$

2.4.2. Determination of the gain of an observer Luenberger by the analytical method

It is desired that the poles have the following values s1 = −160 and s1 = −75, then the characteristic polynomial:

Let us calculate the polynomials characteristic of the observer $P_1(A\text{-}K_1C_1)$ and $P_2(A\text{-}K_2C_2)$

• For the characteristic polynomial $P_1(A\text{-}K_1C_1)$

$$\begin{cases} C_1 = \begin{bmatrix} \dfrac{1}{L} & 0 \end{bmatrix} = [200 \quad 0] \\ \\ K_1 = \begin{bmatrix} k_{11} \\ k_{12} \end{bmatrix} \end{cases} \rightarrow A - K_1C_1 = \begin{bmatrix} -200 - 200k_{11} & -200 \\ 40 - 200k_{12} & -0.1 \end{bmatrix}$$

$$\det(sI - (A - K_1C_1)) = \begin{bmatrix} s + 200 + 200k_{11} & 200 \\ -40 + 200k_{12} & s + 0.1 \end{bmatrix} = s^2 + (200.1 + k_{11})s + 8020 + 40000k_{22}$$

$$\rightarrow \begin{cases} 200k_{21} + 200.1 = 235 \\ 40000k_{22} + 8020 = 12000 \end{cases} \rightarrow \begin{cases} k_{11} = 0.1745 \\ k_{12} = -0.099 \end{cases}$$

- For the characteristic polynomial $P_2(A-K_2C_2)$

$$\begin{cases} C_2 = \begin{bmatrix} 0 & \dfrac{1}{J} \end{bmatrix} = \begin{bmatrix} 0 & 1000 \end{bmatrix} \\ K_1 = \begin{bmatrix} k_{21} \\ k_{22} \end{bmatrix} \end{cases} \rightarrow \det(sI - (A - K_2C_2)) = \begin{bmatrix} s + 200 & 200 + 1000k_{21} \\ -40 & s + 0.1 + 1000k_{22} \end{bmatrix}$$

$$\rightarrow \begin{cases} k_{21} = -0.0750 \\ k_{22} = 0.0349 \end{cases}$$

2.4.3. Determination the gain of a Luenberger observer by bond graph model

Using the theorem of Rahmani [6]:

- The coefficient a_1 is equal to the total gain of families of first order causality cycles in the jump graph model of **Figure 8**.

- The coefficient a_2 is equal to the total gain of second-order families of the causation cycles in the jump graph model of **Figure 8**.

To calculate the gains k_{11} and k_{12}, it is necessary to use **Table 1** that indicates the causality cycles in the observer's bond graph model.

- For the BGO1 model

The coefficient a1 is equal to the sum of the gains of the first order:

$a_1 = G_1 + G_2 + G_3$

$$200\,k_{11} = a_1 - (R/L) + (b/J) = 235 - (200 + 0.1)$$

So $k_{11} = 0.1745$.

To calculate k_{12}, it is necessary to determine the coefficient of a_2 (a_2 equal to the sum of the gains of the second order):

- For the BGO2 model

The coefficient a1 is equal to the sum of the gains of the first order:

$a_1 = G_1 + G_2 + G_4$

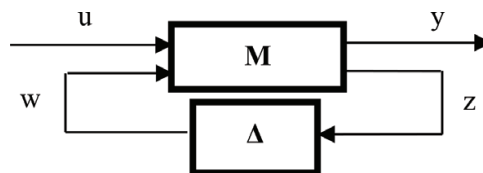$$1000\,k_{22} = a_1 - (R/L) + (b/J) = 235 - (200 + 0.1)$$

So $k_{22} = 0.0349$

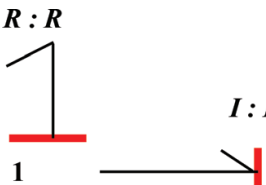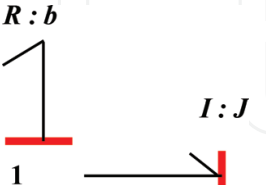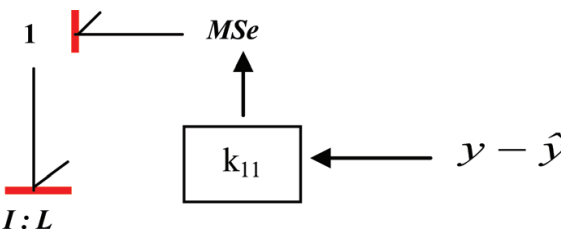**Figure 8.** Schema of the LFT principle.
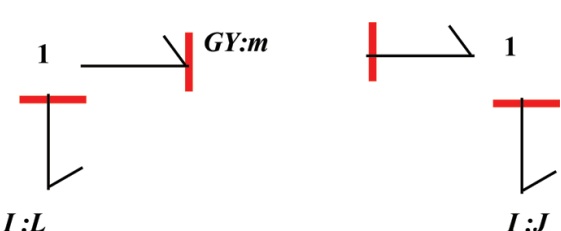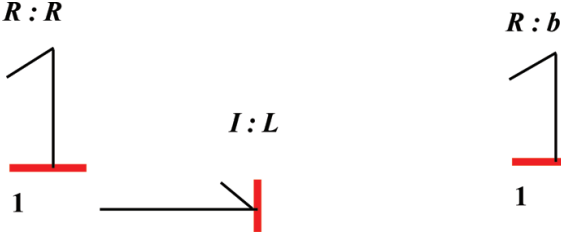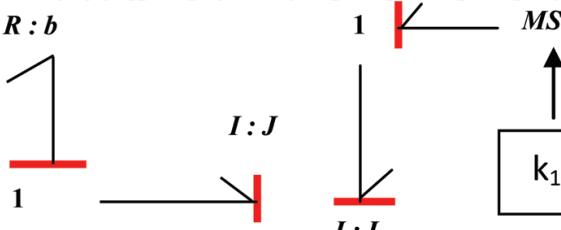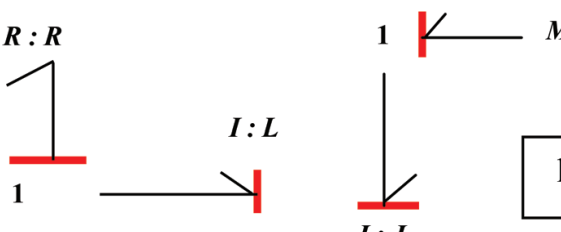
First order of the causation cycle	Gain
R : R **I : L** **1**	$G_1 = (-1)(-R/Ls)$
R : b **I : J** **1**	$G_2 = (-1)(-b/Js)$
1 MSe k_{11} ← $y - \hat{y}$ **I : L**	$G_3 = (k_{11})(1/Ls)$

Second order of causality cycle	Gain
1 GY:m **1** **I :L** **I :J**	$G_4 = (m^2/JLs^2)$
R : R **I : L** **1** **R : b** **I : J** **1**	$G_5 = (Rb/JLs^2)$
R : b **I : J** **1** **1** MSe **I : L** k_{11} ← $y - \hat{y}$	$G_6 = (bk_{11}/JLs^2)$
R : R **I : L** **1** **1** MSe k_{12} ← $y - \hat{y}$ **I : J**	$G_7 = (Rk_{12}/JLs^2)$

Table 1. Causation cycles in the bond graph model of observers BGO1 and BGO2.

Causal of order i	Family of cycles	
	Total gain in BGO1	Total gain in BGO2
1	200.1 + 200 k_{11}	200.1 + 1000 k_{22}
2	8020 + 20 k_{11} + 4000 k_{12}	8020 + 40,000 k_{21} + 200,000 k_{22}

Table 2. Total gains of families of causal cycles in the bond graph model of observers BGO_1 and BGO_2.

To calculate k_{21}, it is necessary to determine the coefficient of a_2 (a_2 equal to the sum of the gains of the second order):

$$a_2 = G_5 + G_6 + G_8 + G_{10} = \left(m^2/JL\right) + (Rb/JL) + (mk_{21}/JL) + (Rk_{22}/JL)$$

So
$$k_{21} = JL\left(a_2 - \left[\left(m^2/JL\right) + (Rb/JL) + k_{22}(R/JL)\right]\right)/m = -0.0750$$

Table 2 represents the total earnings of i-order causal cycle families in the first and second observer graph (BGO1 and BGO2).

3. Robust diagnosis using bond graph model

3.1. Introduction

The diagnosis of industrial systems with uncertain parameters has been studied by several researchers in recent years. Indeed, the method most used is the method of the form linear fractional transformations (LFT), this method offers several advantages such as the flexibility of the diagnosis point of view that allows to model all the uncertainties. But unfortunately, the transition to the LFT form is not always possible (e.g., the nonlinear state models) because the separation of the nominal part from its uncertain part is very difficult (even impossible). Djeziri [7] opted for bond graph modeling using the LFT form method, using a single leap graph model in LFT form generates residuals and adaptive thresholds of normal operation with perfect separation.

3.2. Building a bond graph

Two methods are proposed by Dauphin-Tanguy [8] and Sié Kam [9] to construct parametric uncertainties by BG. The first is to represent uncertainty on a leap graph element as another element of the same type, causally related to the nominal element or the rest of the model. These uncertainties are kept in derived causality when the model is in integral preferential causality so as not to modify the order of the model. The second method is linear fractional transformation (LFT) introduced on mathematical models by Redheffer [10].

3.3. Representation LFT

Linear fractional transformations (LFTs) are widely used in the modeling of uncertain systems. The universality of LFT is due to the fact that any rational expression can be written in this

form according to Alazard [11]. This form of representation is widely used for the synthesis of the control laws of uncertain systems using the principle of µ-analysis. It consists of separating the nominal part of a model from its uncertain part as illustrated in **Figure 8**.

The nominal values are grouped in an augmented matrix denoted M, supposed to be proper, and the uncertainties whatever their type (structured and unstructured parametric uncertainties, modeling uncertainties, measurement noises, etc.) are combined in a matrix Δ of structure diagonal. In the linear case, this standard form leads to a state representation of the form (**Figure 8**):

$$\dot{x} = A \cdot x + B_1 \cdot w + B_2 \cdot u$$
$$z = C_1 \cdot x + D_{11} \cdot w + D_{12} \cdot u \qquad (23)$$
$$y = C_2 \cdot x + D_{21} \cdot w + D_{22} \cdot u$$

- $x \in R^n$: the state vector of the system;

- $u \in R^m$: the vector combining the control inputs of the system;

- $y \in R^p$: the vector grouping the measured outputs of the system;

- $w \in R^l$ and $z \in R^l$: group respectively the inputs and the auxiliary outputs;

- n, m, l and p are positive integers.

The matrices $(A, B_1, B_2, C_1, C_2, D_{11}, D_{12}, D_{21}, D_{22})$ are matrices of suitable dimensions.

3.4. Formatting assumptions LFT

Forming LFT requires that the model be clean and observable [12]. The bond graph methodology allows by causal manipulations to check these properties directly on the bond graph model.

Property 1: A leap graph is unique if and only if it contains no derivative causal dynamic component when it is a preferential integral causality, and reciprocally.

Property 2: A leap graph is structurally observable if and only if the following conditions are met:

- On the bond graph model in integral causality, there exists a causal path between all dynamic elements I and C in integral causality and a detector De or Df;

- All dynamic elements I and C admit causality derived on the leap graph model in preferential derived causality. If dynamic elements I or C remain in integral causality, the dualization of detectors De and Df must make it possible to put them into derivative causality.

3.5. Modeling of BG elements by LFT

The modeling of linear systems with uncertain parameters has been developed in Djeziri's thesis [13], the modeling of uncertain graph leap elements (R, I, C, TF and GY) has been determined. We will therefore limit ourselves in this section to show the two methods of modeling uncertain BG elements, as well as the advantages of BG-LFT for robust diagnosis.

3.5.1. BG element with a multiplicative uncertainty

The introduction of a multiplicative uncertainty on, for example, the element R in causality resistance gives Eq. (25):

$$e_R = R_n \cdot (1 + a_R) \cdot f_R = R_n \cdot f_R + a_R \cdot R_n \cdot f_R = e_n + a_R \cdot e_n = e_n + e_{inc} \qquad (24)$$

- R_n: The nominal value of the R element;

- a_R: The multiplicative uncertainty on the parameter;

- e_R and f_R: represent the force and the flux in the element R, respectively;

- e_n and e_{inc}: represent respectively the effort provided by the nominal parameter and the effort introduced by the multiplicative uncertainty.

The bond graph model equivalent to the mathematical model of Eq. (24) is given in **Figure 9**.

3.5.2. Construction of a BG-LFT model

The complete BG-LFT model is represented by the diagram in **Figure 10**.
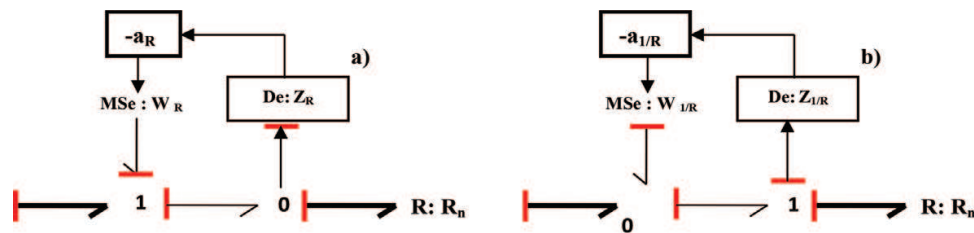

Figure 9. (a): Model BG-LFT of an element R causality resistance with multiplicative uncertainty, (b): Model BG-LFT of an element R with conductance causation with multiplicative uncertainty.
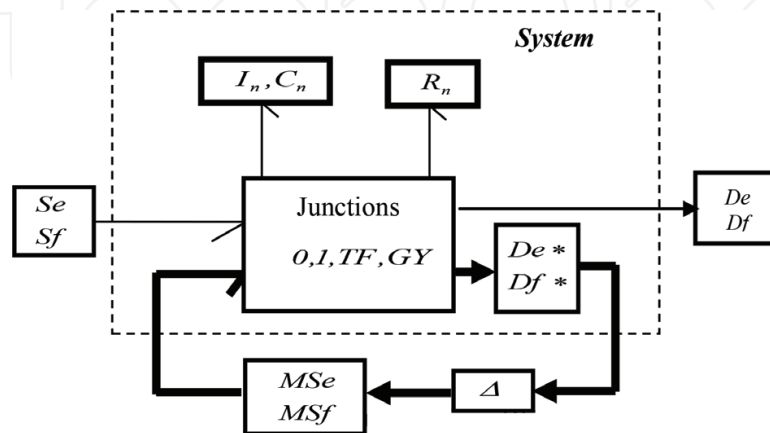

Figure 10. Representation in form BG-LFT.

3.5.3. Rugged diagnosis by ARRs

The generation of robust analytical redundancy relationships (ARRs) from a clean, observable and overdetermined leap graph is summarized by the following steps:

Step 1: Checking the state of the coupling on the model graph deterministic preferential derived causality; if the system is overdetermined, then proceed with the following steps;

Step 2: The leap graph template is set to LFT;

Step 3: The symbolic expression of the RRA is deduced from the equations at the junctions. This first form will be expressed by:

$$\text{For junction } 0 : \sum b_i \cdot \dot{f}_{inc} + \sum Sf + \sum w_i = 0 \tag{25}$$

$$\text{For junction } 1 : \sum b_i \cdot \dot{e}_{inc} + \sum Se + \sum w_i = 0 \tag{26}$$

With $\sum \dot{S}f$ the sum of the flux sources linked to the junction 0, the $\sum \dot{S}e$ sum of the force sources linked to the junction 1, b $= \pm 1$ according to whether the half-arrow enters or leaves the junction, e_{in} and f_{in} are the unknown variables .

Is the $\sum \dot{w}_i$ sum of the modulated inputs corresponding to the uncertainties on the elements related to the junction.

Step 4: Unknown variables are eliminated by traversing causal paths between detectors or sources and unknown variables;

Step 5: After removing the unknown variables, the uncertain RRAs are in the form:

$$RRA : \Phi\left(\sum \dot{S}e, \sum Sf, De, Df, \sum w_i, R_n, I_n, C_n, TF_n, GY_n\right) \tag{27}$$

TF_n and GY_n are, respectively, the nominal values of the modules of the elements TF and GY, also R_n, C_n and I_n are the nominal values of the elements R, C and I.

3.5.4. Robust diagnosis by Luenberger observer using bond graph

The model BG-LFT of the system with the observer of Luenberger is represented by the diagram in **Figure 11**.

3.5.5. Location of defects per observer bench

A single residue allows the detection of a fault. However, the location of a defect requires a set of structured residues. These residues must be designed to be sensitive to certain defects and insensitive to others. The use of observer banks constructed from only part of the inputs and/or outputs of the system makes it possible to respond to this problem. The symptoms generated are compared with fault signatures.
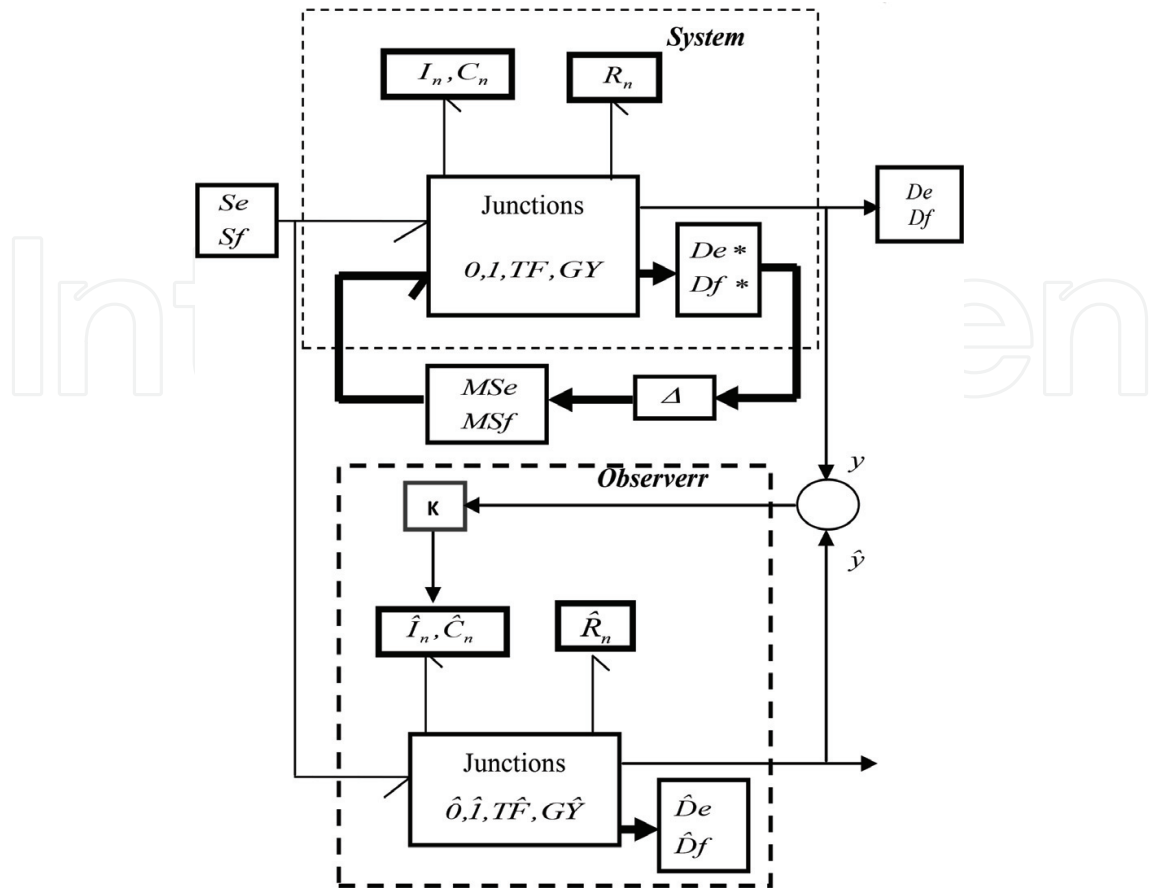
Figure 11. Representation in BG-LFT form of the system with observer from Luenberger.

There are two observer banks:

- The Dedicated Observer Scheme (DOS): the ith observer is controlled by the ith output (input) and all inputs (outputs). The other outputs (inputs) are considered unknown.

- The Generalized Observer Scheme (GOS) structure: the ith observer is controlled by all outputs (inputs) except the ith and all inputs (outputs).

For a given observer bank, the signature of the various defects is defined in the signature table. The rows and columns of this table correspond, respectively, to defects and symptoms. The cells in the table are filled with binary values. A zero (0) means that the symptom is not sensitive to the defect. One (1) means that the symptom is sensitive to this defect.

Figures 12 and **13**, respectively, present the principle of detection and localization of faults by observers (DOS) and (GOS).

Tables 3 and **4** illustrate the signatures of the various defects as a function of the residuals.

3.6. Example

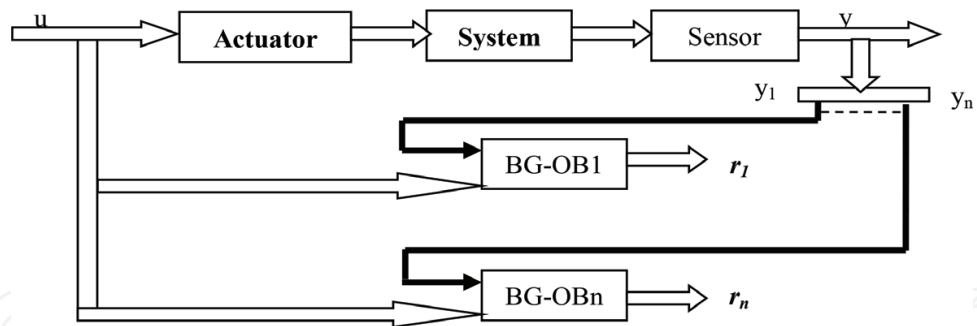Consider the same example (DC motor) given in **Figure 7**.
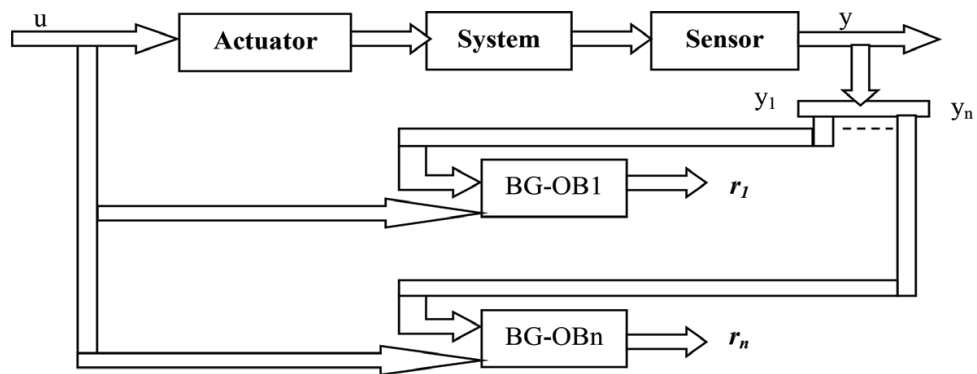
Figure 12. Sensor faults with DOS structure.

Figure 13. Sensor faults with GOS structure.

	F_{s1}	F_{s2}	....	F_{sn}
r_1	1	0	0	0
r_2	0	1	0	0
…	0	0	1	0
r_n	0	0	0	1

Table 3. Signature of sensor faults with DOS structure.

	F_{s1}	F_{s2}	....	F_{sn}
r_1	0	1	1	1
r_2	1	0	1	1
…	1	1	0	1
r_n	1	1	1	0

Table 4. Signature of sensor faults with GOS structure.

3.6.1. Proportional observer diagnosis using the bond graph model

The application of leap graph for the diagnosis of industrial systems is mainly justified by the fact that the model can be fine-tuned by adding or removing jump graph elements (graphically) according to simplifying assumptions. It is therefore also desirable that for the state estimation, the observer design is carried out using graphic methods and taking advantage of the properties.

3.6.2. Requirements

For observer construction, we need to check the following conditions:

The first condition is satisfied: When the bond graph model of the DC motor is put into a preferred integral causality, it is clear that there exists a causal path linking the sensors Df_1 and Df_2 to each dynamic element I in the integral causality (**Figure 14(a)**). The second condition is satisfied: when we put the jump engine model of the DC motor in derived causality, all the elements I admit a derivative causality, and the sensors Df_1 and Df_2 are dualized (**Figure 14(b)**).

3.6.3. Calculation of residues

Figure 15 represents a construction of the proportional observer of the system using the bond graph approach.

We simulated the system with the 20sim software. **Figure 16** shows the evolution of the real and estimated state variables.

From model BG of **Figure 15**, the residues r_1(t) and r_2(t) can be deduced.

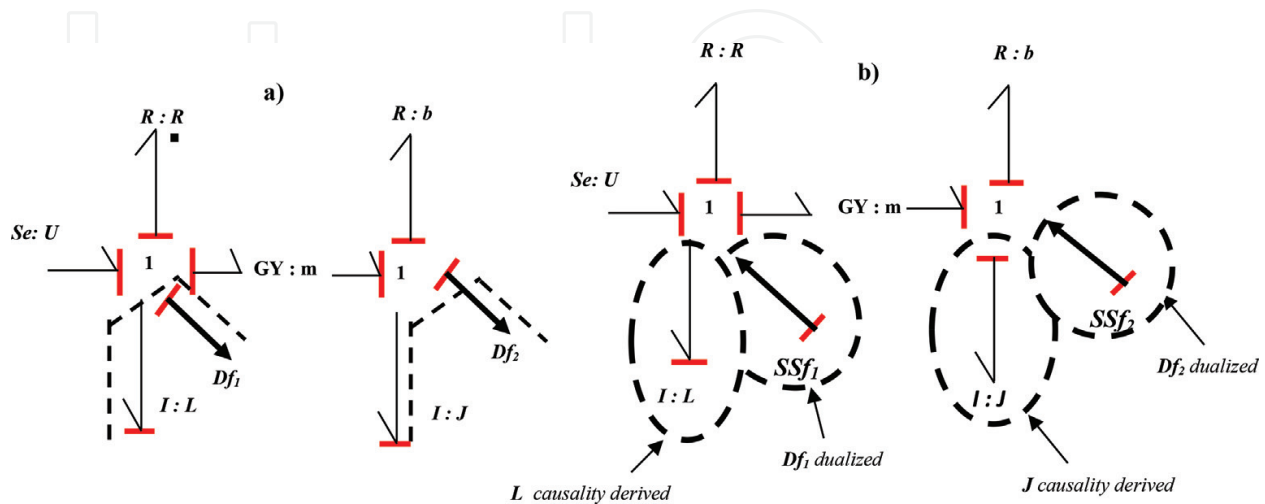Residue r_1: $f_2 - f_{\hat{2}} = Df_2 - f_{\hat{2}} = 0$.

Figure 14. (a): Bond model of the DC motor in integral causality, (b): bond model of the DC motor in derived causality.
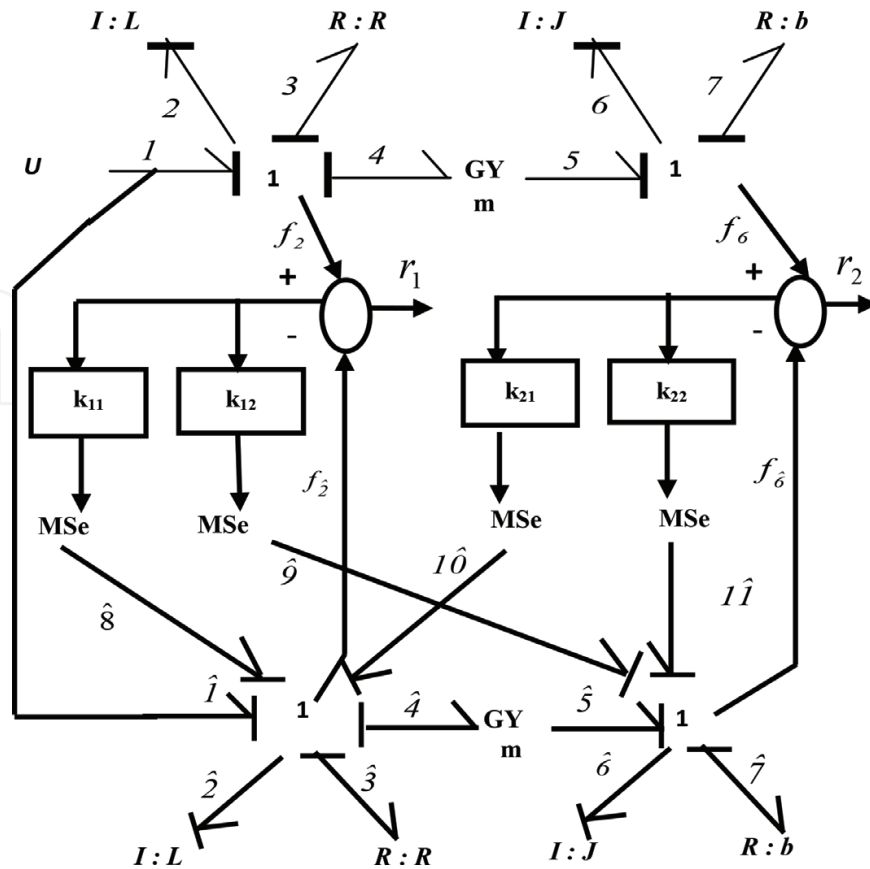
Figure 15. Proportional observer using bond graph of DC motor monitor.

Therefore,

$$r_1(t)\left(m^2Rb + m^2RK_{11} + mK_{12}\right) + \frac{dr_1(t)}{dt}\left(m^2RJ + m^2Lb + m^2LK_{11}\right) + \frac{d^2r_1(t)}{dt}\left(m^2LJ\right)$$
$$+r_2(t)\left(m^2RK_{21} + mK_{22}\right) + \frac{dr_2(t)}{dt}\left(m^2LK_{21}\right) = 0 \tag{28}$$

Residue r_2: $f_6 - f_{\hat{6}} = Df_1 - f_{\hat{6}} = 0$

We proceed in the same way, we end:

$$r_2(t)\left(m^2Rb + m^2bK_{22} + mK_{21}\right) + \frac{dr_2(t)}{dt}\left(m^2RJ + m^2Lb + m^2JK_{21}\right) + \frac{d^2r_2(t)}{dt}\left(m^2LJ\right)$$
$$r_1(t)\left(m^2bK_{12} + mK_{11}\right) + \frac{dr_2(t)}{dt}\left(m^2JK_{12}\right) = 0 \tag{29}$$

Figure 17 shows the convergence of residuals toward zero.

3.6.4. Génération des résidus avec défauts capteurs

The sensors Df_1 and Df_2 are affected by defects (F_{C1} and F_{C2}), then:

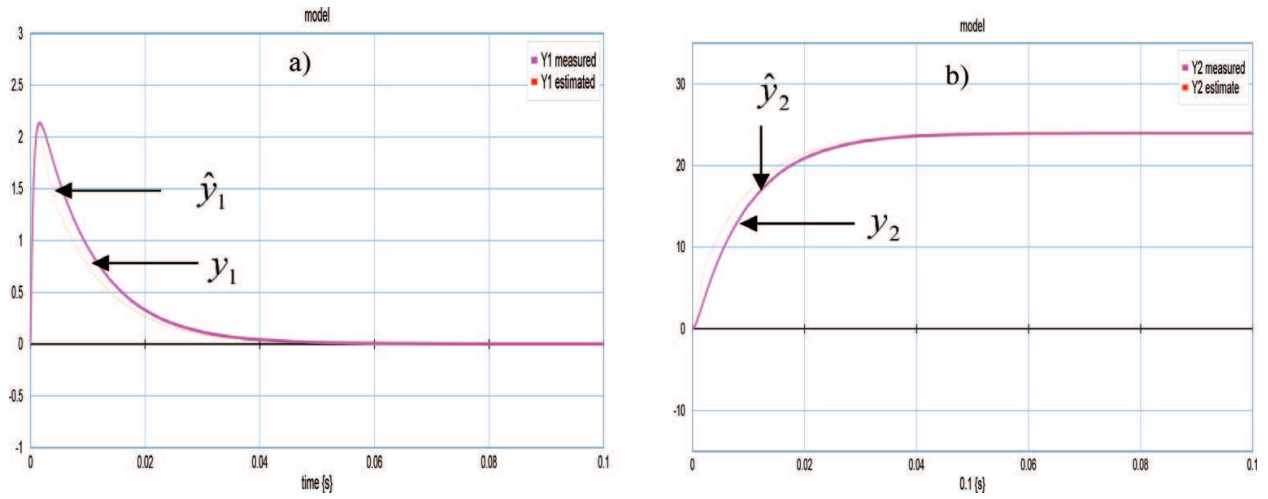Residue r_1: $\left(Df_1 + F_{C1}\right) - f\hat{6} = 0$

Figure 16. Output variables, (a): output variables y_1 and $\hat{y}_1$, (b): output variables y_2 and $\hat{y}_2$.
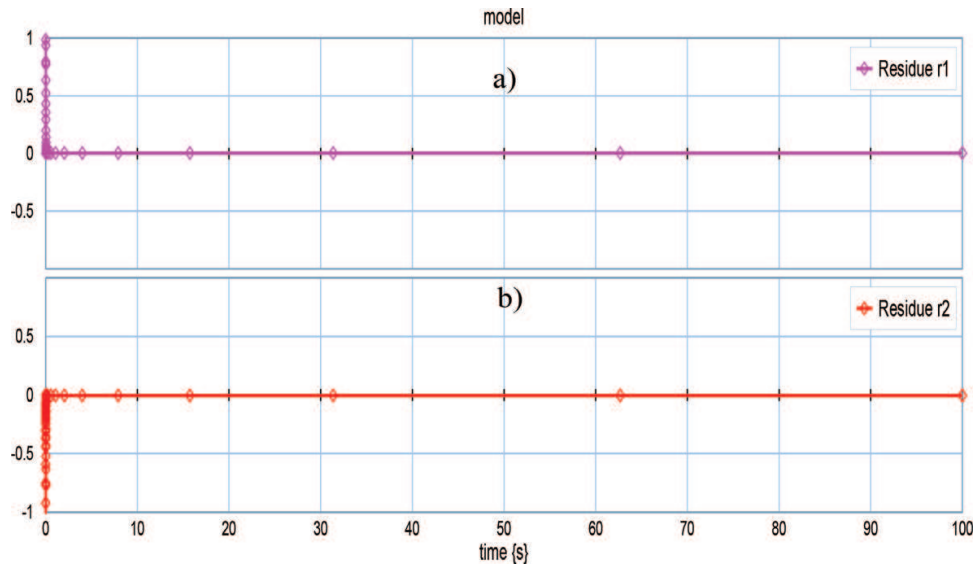

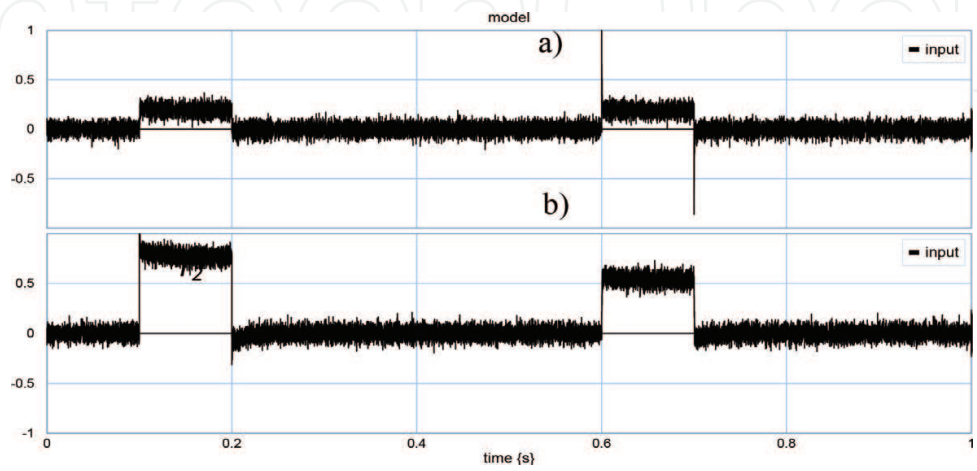**Figure 17.** (a): Residue $r_1(t)$, (b): Residue $r_2(t)$ in the case of normal operation.

Figure 18. (a): Residue $r_1(t)$ with defects of the sensors Df_1 and Df_2, (b): Residue $r_2(t)$ with defects of the sensors Df_1 and Df_2.

$$r_1(t)\left(m^2 Rb + m^2 RK_{11} + mK_{12}\right) + \frac{dr_1(t)}{dt}\left(m^2 RJ + m^2 Lb + m^2 LK_{11}\right)$$

$$+\frac{d^2 r_1(t)}{dt}\left(m^2 LJ\right) + r_2(t)\left(m^2 RK_{21} + mK_{22}\right) + \frac{dr_2(t)}{dt}\left(m^2 LK_{21}\right) = F_{C1}(t)\left(bm^2\right) \quad (30)$$

$$+\frac{dF_{C1}(t)}{dt}\left(Lm^2\right) - F_{C2}(t)(m)$$

Residue r_2: $\left(Df_2 + F_{S2}\right) - f\hat{2} = 0$

$$r_2(t)\left(m^2 Rb + m^2 bK_{22} + mK_{21}\right) + \frac{dr_2(t)}{dt}\left(m^2 RJ + m^2 Lb + m^2 JK_{21}\right)$$

$$+\frac{d^2 r_2(t)}{dt}\left(m^2 LJ\right) + r_1(t)\left(m^2 bK_{12} + mK_{11}\right) + \frac{dr_2(t)}{dt}\left(m^2 JK_{12}\right) = \quad (31)$$

$$F_{C2}(t)\left(bm^2\right) + \frac{dF_{C2}(t)}{dt}\left(Jm^2\right) - F_{C1}(t)(m)$$

Eqs. (30) and (31) show that residues $r_1(t)$ and $r_2(t)$ are sensitive to sensor defects. **Figure 18** confirms the sensitivity of the residuals to the defects of the sensors Df_1 and Df_2.

3.6.5. Robust diagnosis by observer from Luenberger

Figure 19 shows the Luenberger observer of the DC motor using the BG-LFT model.

From the BG-LFT model (**Figure 19**), residues $R_1(t)$ and $R_2(t)$ can be deduced.

Residue R_1: $f_2 - f_{\hat{2}} = 0$

$$\left[r_1(t)\left(m^2 Rb + m^2 RK_{11} + mK_{12}\right) + \frac{dr_1(t)}{dt}\left(m^2 RJ + m^2 Lb + m^2 LK_{11}\right)\right.$$

$$+\frac{d^2 r_1(t)}{dt}\left(m^2 LJ\right) + r_2(t)\left(m^2 RK_{21} + mK_{22}\right) + \left.\frac{dr_2(t)}{dt}\left(m^2 LK_{21}\right)\right] \quad (32)$$

$$-\left[w_J(t)\left(m^2 R_n\right) + \frac{dw_J(t)}{dt}\left(m^2 L_n\right) + w_L(t)(m)\right] = 0$$

Eq. (32) is composed of two parts: the first part corresponds to the evolution of the normal residue (r_{1n}) and the second part represents the evolution related to the uncertainty of the parameters (d_1).

$$\begin{cases} R_1 = r_{1n} + d_1 \\ r_{1n} = [r_1(t)\left(m^2 Rb + m^2 RK_{11} + mK_{12}\right) + \frac{dr_1(t)}{dt}\left(m^2 RJ + m^2 Lb + m^2 LK_{11}\right) \\ +\frac{d^2 r_1(t)}{dt}\left(m^2 LJ\right) + r_2(t)\left(m^2 RK_{21} + mK_{22}\right) + \frac{dr_2(t)}{dt}\left(m^2 LK_{21}\right)] \\ |d_1| = w_J(t)\left(m^2 R_n\right) + \frac{dw_J(t)}{dt}\left(m^2 L_n\right) + w_L(t)(m) \end{cases}$$
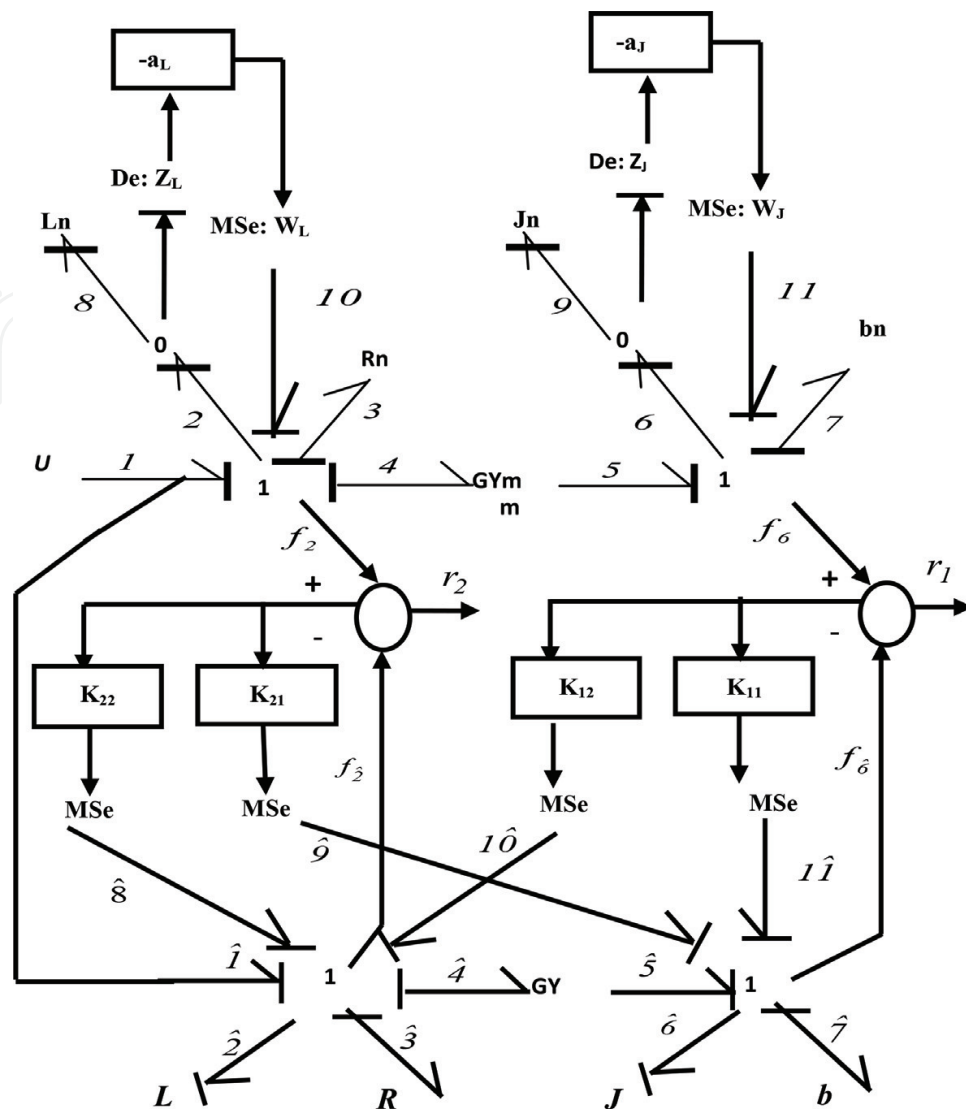
Residue R_2: $f_6 - f\hat{6} = 0$

Figure 19. Luenberger observer of the DC motor using the BG-LFT model.

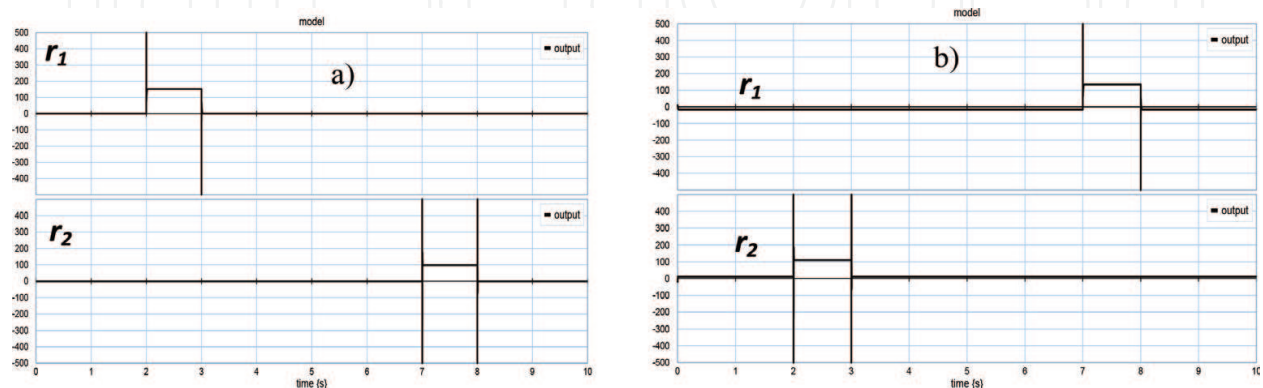**Figure 20.** (a): Residue $r_1(t)$ and $r_2(t)$ for the DOS structure, (b): residue $r_1(t)$ and $r_2(t)$ for the DOS structure.

Structure DOS			Structure GOS		
	Df_1	Df_2		$Df1$	$Df2$
r_1	1	0	r_1	1	0
r_2	0	1	r_2	0	1

Table 5. Signatures of faults. (a) Structure DOS and (b) structure GOS.

$$[r_2(t)(m^2Rb + m^2bK_{22} + mK_{21}) + \frac{dr_2(t)}{dt}(m^2RJ + m^2Lb + m^2JK_{21})$$

$$+ \frac{d^2r_2(t)}{dt}(m^2LJ) + r_1(t)(m^2bK_{12} + mK_{11}) + \frac{dr_2(t)}{dt}(m^2JK_{12})] \tag{33}$$

$$- [w_L(t)(m^2b_n) + \frac{dw_L(t)}{dt}(m^2J_n) + w_j(t)m = 0$$

Eq. (33) is composed of two parts: the first part corresponds to the evolution of the normal residue (r_{2n}) and the second part represents the evolution related to the uncertainty of the parameters (d_2).

$$\begin{cases} R_2 = r_{2n} + d_2 \\ r_{2n} = r_2(t)(m^2Rb + m^2bK_{22} + mK_{21}) + \frac{dr_2(t)}{dt}(m^2RJ + m^2Lb + m^2JK_{21}) \\ \quad + \frac{d^2r_2(t)}{dt}(m^2LJ) + r_1(t)(m^2bK_{12} + mK_{11}) + \frac{dr_2(t)}{dt}(m^2JK_{12})] \\ |d_2| = w_L(t)(m^2b_n) + \frac{dw_L(t)}{dt}(m^2J_n) + w_j(t)m \end{cases}$$

3.6.6. Detection and localization of sensor faults

Figure 20 shows the evolution of residues based on the BG model using the BG-DOS and BG-GOS structures, the residue $r_1(t)$ is sensitive to the defects occurring on the Df_1 sensor while the residue $r_2(t)$ is sensitive to faults on the Df_2 sensor.

Table 5(a) and **(b)** represents the binary signatures of the defects for the deduced DOS and GOS structures to perfectly isolate the defects.

4. Conclusion

In this chapter, we proposed a technique for the diagnosis of linear systems by Luenberger observer using the leap graph. We presented the leap graph approach for constructing a full-order observer and proposed a new BG-based observer method. Subsequently, we presented the systems with uncertain parameters modeled by the leap graph approach and we also proposed a new method of diagnosis of systems with uncertain parameters by Luenberger observer.

In the last part of this chapter, we developed and proposed an observer-based diagnostic technique (BG-DOS / BG-GOS) to detect and locate faults.

Author details

Abderrahmène Sallami

Address all correspondence to: abderrahmenesallami@gmail.com

Department of Electrical Engineering, Laboratory ACS, Tunisia

References

[1] Khedher A, Othman KB, Benrejeb M, Maquin D. Adaptive observer for fault estimation in nonlinear systems described by a Takagi-Sugeno model. In: 18th Mediterrranean Conference on Control and Automation, Marrakech, Morocco; 2010. pp. 23-25

[2] Maquin D, Ragot J. Diagnostic Des Systèmes Linéaires. Hermes ed. Paris, France: Hermes; 2000

[3] Sueur C, Dauphin-Tanguy G. Structural Controllability and Observability of linear Systems Represented by Bond Graphs. Journal of the Franklin Institute. 1989;**326**:869-883

[4] Pichardo-Almarza C, Rahmani A, Dauphin-Tanguy G, Delgado M. Observateur Proportionnel-Intégral pour des Systèmes Linéaires Modélisés par Bond Graphs. In: Actes des Journées Doctorales d'Automatique; 2003

[5] Luenberger DG. An introduction to observers. IEEE Transactions on Automatic Control. 1971;**16**:596-602

[6] Rahmani A, Sueur C, Dauphin-Tanguy G. Pole assignment for systems modelled by bond graph. Journal of the Franklin Institute. 1994;**331**(3):299-312

[7] Djeziri MA, Ould Bouamama B, Merzouki R. Modelling and robust FDI of steam generator using uncertain bond graph model. Journal of Process Control. 2009;**19**:149-162

[8] Dauphin-Tanguy G, Sié Kam C. How to Model Parameter Uncertainies in a Bond Graph Framework. Erlangen, Germany: ESS'99; 1999. pp. 121-125

[9] Sié Kam C, Dauphin-Tanguy G. Bond graph models of structured parameter uncertainties. Journal of the Franklin Institute. 2005;**342**:379-399

[10] Redheffer R. On a certain linear fractional transformation. Journal of Mathematics and Physics Banner. 1960;**39**:269-286. l'aide d'éléments caractérisés». 8ème colloque Electronique dePuissance du Futur EPF 2000, Lille; 2000

[11] Alazard D, Cumer C, Apkarian P, Gauvrit M, Fereres G. Robustesse et Commande Optimale. Cépadues ed. 1999. ISBN: 2.85428.516.6

[12] Sié Kam C. Les bond graphs pour la modélisation des systèmes linéaires incertains [Thèse de doctorat]. USTLille1-ECLille; Décembre 2001. N°d'ordre 3065, 2001

[13] Djeziri MA. Diagnostic des systèmes incertains par l'approche bond graph [thèse de doctorat]. École Centrale de Lille; 2007